

# Contrast variation SANS investigation of composition distributions in mixed surfactant micelles

メタデータ	言語: eng 出版者: 公開日: 2022-03-11 キーワード (Ja): キーワード (En): 作成者: メールアドレス: 所属:
URL	<a href="https://doi.org/10.24517/00065559">https://doi.org/10.24517/00065559</a>

This work is licensed under a Creative Commons Attribution-NonCommercial-ShareAlike 3.0 International License.



# Contrast Variation SANS Investigation of Composition Distributions in Mixed Surfactant Micelles

Mats Almgren,<sup>\*,†</sup> Vasil M. Garamus,<sup>‡</sup> Tsuyoshi Asakawa,<sup>§</sup> and Nan Jiang<sup>†</sup>

Department of Physical and Analytical Chemistry, Uppsala University, P.O. Box 579, SE-751 23 Uppsala, Sweden, GKSS Research Centre, Max-Planck-Strasse, 21502 Geesthacht, Germany, and Department of Chemistry and Chemical Engineering, Kanazawa University, Kanazawa 920-8667, Japan

Received: January 12, 2007; In Final Form: April 24, 2007

Small angle neutron scattering measurements have been performed on three systems (HFDeP-d5-C (N-1(1,1,2,2-tetrahydroperfluorodecanoyl)pyridinium-d5 chloride)/C<sub>16</sub>PC in 63 mM NaCl; HFDeP-d5-C/C<sub>12</sub>PC in 200 mM NaCl, and as an example of an ideally mixed system, SDS/SDS-d25 in 200 mM NaCl) containing micelles formed in a binary mixture of surfactants, in order to investigate the composition distribution of the mixed micelles. The experimental data were collected varying the contrast between the average scattering length density of micelles and aqueous solvent by changing the H<sub>2</sub>O/D<sub>2</sub>O ratio. Analysis of data includes a model-independent approach—the indirect Fourier transformation method and direct modeling—simultaneous fit at all contrasts by the scattering from micelles of equal size and shape with composition distribution and an effective interaction. It has earlier been shown (Almgren, M.; Garamus, V. M. *J. Phys. Chem. B* 2005, 109, 11348) that for micelles of equal size, independent of the composition, and with negligible intermicellar interactions, the scattered intensity at zero angle varies quadratically with the contrast, with the minimum intensity at the nominal match point proportional to  $\sigma^2$ , the variance of the micelle composition distribution. Within the regular solution framework, the composition distribution and its variance are uniquely defined by the value of the interaction parameter and the micelle aggregation number. At 25 °C, the first system gave  $\sigma = 0.37$ , corresponding to a broad, bimodal composition distribution, the second  $\sigma = 0.22$ , a broad distribution with a shallow minimum at the midpoint. For SDS/SDS-d25, we found  $\sigma = 0.006 \pm 0.030$ , which is a smaller value than that of the binominal composition distribution expected for an ideally mixed system.

## Introduction

Micelle formation by mixtures of surfactants has attracted considerable attention.<sup>1–5</sup> Quantitative treatments of such systems have usually been made within a regular solution framework, with reasonable success. The regular solution approach relates the concentrations of free surfactants,  $c_i$ , to the composition of the micelles,  $\bar{x}_i$ ,

$$c_i = c_i^\circ f_i \bar{x}_i; \quad i = 1, 2 \quad (1)$$

where  $c_i^\circ$  is the critical micelle concentration (cmc) of surfactant  $i$ . The activity factor,  $f_i$ , is given by

$$\ln f_i = \alpha(1 - \bar{x}_i)^2 \quad (2)$$

where  $\alpha$  is the interaction parameter. Although the terminology is confused, eq 2 is often taken to define a regular solution; we will follow this practice.

The regular solution equations follow from various molecular models, in particular lattice models, as well as by an empirical approach as a “first step” from the ideal solution.<sup>6</sup> The important characteristics are that the entropy of mixing is that of an ideal mixture, that is, independent of the interactions between the molecules, and that the interaction parameter,  $\alpha kT$ , is the

increase in energy when a molecule from pure liquid of “1” is exchanged for a molecule from the pure liquid of “2”.

In applications to micellar systems, it is natural to regard the surfactants as forming a two-dimensional lattice (closed to a sphere for globular micelles). Lattice models that give regular solution behavior, such as the Bragg–Williams model,<sup>7</sup> usually consider only nearest neighbor interactions, and the interaction parameter is given by

$$\alpha \equiv \frac{zw}{kT} \quad (3)$$

where  $w$  is the excess interaction energy between two unlike neighbors and  $z$  is the number of nearest neighbors.

In ideal mixing, the interaction parameter is zero and the activity coefficients unity, and the model reduces to the ideal mixing model first proposed by Clint.<sup>8</sup> Note that there is no reference to the size of micelles; only the average composition of the micelles is involved. The micelles are looked upon as a pseudophase, an infinite two-dimensional lattice, in equilibrium with the surrounding aqueous solution.<sup>9</sup>

As the micellar pseudophase is subdivided into individual micelles, another consequence of the interactions between the surfactants becomes apparent. The distribution of the surfactants over the micelles, the micelle composition distribution, will depend on the interaction between the surfactants. This distribution problem has been much less discussed than the effects of the nonideality on the distribution between micellar and aqueous pseudophases. It is important experimentally in connection with

\* Corresponding author. E-mail: Almgren@fki.uu.se.

† Uppsala University.

‡ Max-Planck-Strasse.

§ Kanazawa University.

fluorescence quenching in micelles. With one of the surfactants serving as a fluorescence quencher, the interactions will cause the quenching to depart from the behavior expected from a random distribution of quenchers over the micelles.<sup>6,10,11</sup>

For the simplest case of micelles with the same total aggregation number independent of composition, the distribution of the two surfactants over the micelles is binominal when the excess interaction energy is zero in the ideal mixing case. At a total aggregation number of 100, and a 50:50 average composition, the width of the composition distribution should be  $\sigma = 0.05$  (and larger for smaller micelles). Nonideally mixed systems with attractive interactions between the surfactants would have more narrow composition distributions, and repulsive interactions such as between fluorinated and hydrogenous surfactants would lead to a broadening. In the hypothetical case of complete demixing into pure surfactant micelles of the two types, the width should reach a maximum value of  $\sigma = 0.5$ . A square composition distribution with all compositions between 0 and 1 equally probable has  $\sigma = 0.289$  and represents the broadest possible monomodal distribution. The scale from  $\sigma \approx 0.05$  to 0.5 thus encompasses binary mixed surfactant micelles from ideally mixed to completely demixed. This is of interest, since  $\sigma$  may be obtained from contrast variation small angle neutron scattering experiments, as will be detailed below.<sup>12</sup>

Micellization in mixtures of normal and fluorinated surfactants has attracted special attention ever since Murkerjee and Mysels suggested in 1975 that a demixing may occur, leading to coexisting micelles enriched in one or the other of the surfactants.<sup>13</sup> In the regular solution model, demixing would set in above a critical value,  $\alpha = 2$ , of the interaction parameter. Numerous experiments have been performed since then designed to settle the question if or to what extent such a demixing occurs in various systems. The literature has been reviewed and discussed critically.<sup>12,14–17</sup> Small angle neutron scattering (SANS) with contrast variation by using D<sub>2</sub>O/H<sub>2</sub>O mixtures for solvent would, at a first glance, appear ideally suited for such studies: one solvent mixture would make one type of micelles invisible, another the other type, and a scattered intensity would remain for the demixed system at the nominal match point where the scattering length density of the mixed surfactants equals that of the solvent mixture. At this point, the scattering would all but disappear for an ideally mixed system. Only few studies of this kind have been made. The conclusions from the early studies<sup>18–21</sup> were in all cases that no demixing occurred in the systems selected, whereas such evidence was found more recently in mixtures of HFD<sub>5</sub>PC (*N*-1(1,1,2,2-tetrahydroperfluorodecanoyl)pyridinium chloride) and C<sub>16</sub>TAC (hexadecyltrimethyl ammonium chloride).<sup>12,15</sup>

When the composition distribution of mixed micelles is the main issue, it is difficult to apply the standard modeling techniques that have been used successfully in SANS studies of various micellar systems.<sup>22,23</sup> In the conventional approach, the interactions between the micelles are accounted for within the decoupling approximation,<sup>22,24</sup> assuming that the interactions are neither correlated to the orientation (for non-isotropic particles) nor correlated to the size polydispersity. Size polydispersity is described by the convenient two-parameter Schultz distribution. The micelles are assumed to have a tractable shape, usually spherical, oblate, or prolate, and the internal scattering length density distribution is approximated by a core–shell model.<sup>23,25,26</sup> For mixed micelles, the possibility of a composition distribution has been considered but at best taken care of as a small correction valid for a narrow distribution.<sup>27,28</sup> A method to determine the average composition of the mixed micelles

from contrast variation measurement has been devised, which is useful when the concentrations of free surfactants are unknown but not negligible.<sup>27,28</sup> In the few studies designed to investigate micellar demixing, however, the information has not been sought from direct modeling but has been extracted from the variation of  $I(q)$ , the scattered intensity extrapolated to  $q = 0$ , with the contrast.<sup>18–21</sup> The extrapolation has been made in plots of  $\ln I(q)$  versus  $q^2$ , that is, from the Guinier regime. No physically motivated analytical expression that could be employed in direct modeling is available for the composition distribution, not even for constant aggregation numbers, and with a covariation of composition and size, the situation is even more complex. Faced with that problem, we have found it virtually impossible to directly use a modeling approach and have resorted to an initial analysis of the  $I(0)$  values. Since we are primarily interested in the composition distribution and not the details of the micellar structure, it is a strength to get model-independent information of the distribution, even if it is approximate. Instead of an extrapolation from the Guinier regime, we chose to determine the  $I(0)$  values from an indirect fourier transformation (IFT) analysis<sup>29</sup> using data obtained in the presence of added salt to reduce the electrostatic interactions. We have still to be concerned, however, about the possibility of a change in size and shape with the composition, and about residual micelle interactions. Guided by the results from the initial analysis, we have performed some modeling, including intermicellar interactions on the level of effective hard-sphere interactions. By this modeling, we have tested the consistency of the results and estimated the magnitude of possible composition-dependent size variations.

For non-interacting globular particles of the same size but different compositions, the zero angle SANS intensity depends on the scattering length density of the solvent mixture according to eq 4.<sup>12,30</sup>

$$\frac{d\Sigma}{d\Omega}(0) = n_m V_m^2 [\sigma^2 (\rho_{FS} - \rho_{HS})^2 + (\bar{\rho} - \rho_S)^2] \quad (4)$$

$(d\Sigma/d\Omega)(0)$  is the scattering cross section at the modulus of the scattering vector,  $q = 0$ ,  $n_m$  is the number density of micelles,  $V_m$  is the micelle volume,  $\rho$  is the scattering length density, with subscript FS for fluorinated surfactant, HS for hydrogenous surfactant, and S for solvent, and  $\bar{\rho}$  represents the scattering length density of the (hypothetical) fully mixed micelle.  $\sigma$  is the width of the micelle composition distribution,  $f(x_F)$ , and is given by

$$\sigma^2 = \int_0^1 (x_F - \bar{x}_F)^2 f(x_F) dx_F \quad (5)$$

where  $x_F$  is the mole fraction of fluorinated surfactant in a micelle. The expression is valid for non-interacting globular particles of equal size, or possibly a narrow size distribution that is not correlated to the composition distribution. Since only the scattering at  $q = 0$  is involved, the scattering length density distribution within the particles has no influence. For micelles of a fixed composition, eq 4 reduces to the usual expression with zero scattering at the contrast match point between solvent and micelles.<sup>18</sup>

Equation 4 was applied to results for a mixture of a partially fluorinated cationic surfactant with a deuterated headgroup, HFD<sub>5</sub>P-d<sub>5</sub>-C (*N*-1(1,1,2,2-tetrahydroperfluorodecanoyl)pyridinium-d<sub>5</sub> chloride), and C<sub>16</sub>TAC (cetyltrimethylammonium chloride).<sup>12</sup> Since the surfactants are ionic, salt was added to reduce the electrostatic interactions, and the surfactant concentrations were kept low (slightly more than 1 vol % surfactant)

to further reduce intermicellar interactions. Measurements were performed in six D<sub>2</sub>O/H<sub>2</sub>O solvent mixtures, with the mole fraction of D<sub>2</sub>O varying from 0.05 and 1.0. The data were analyzed by IFT<sup>29</sup> using results for  $q > 0.02 \text{ \AA}^{-1}$ , where the effect of intermicellar interactions is small. The zero angle scattering intensities obtained from this analysis gave a very good fit to eq 4 and resulted in values of  $\sigma = 0.33$  at 25 °C and 0.20 at 60 °C for this system. The low temperature composition distribution is thus too broad to be monomodal, and a demixing into two micelle populations occurs. At the higher temperature, the distribution of compositions is still broad, but it is not necessarily bimodal.

In this contribution, we report on the results for three new systems. In order to ascertain that the excess interactions between the different surfactants in the micelles are due only to the interactions between the fluorocarbon and hydrocarbon tails, we chose a hydrogenous surfactant with the same headgroup as the fluorinated one, cetylpyridinium chloride (C<sub>16</sub>-PC). In the second system, the hydrogenous surfactant had a shorter alkyl chain, dodecyl pyridinium chloride (C<sub>12</sub>-PC). This will reduce the repulsive interactions, and it is not certain that a bimodal composition distribution will be obtained. Third, a system with ideal mixing behavior was selected, SDS and its perdeuterated analogue SDS-d25. The determined width of the composition distributions will be discussed with reference to the composition distributions expected from regular solution treatments. The direct modeling will be reported in a separate section.

## Experimental Section

**Materials.** The cationic fluorocarbon surfactant HFDeP-d5-C was synthesized as described.<sup>31</sup> Cetylpyridinium chloride (C<sub>16</sub>-PC, Merck) and dodecyl pyridinium chloride (C<sub>12</sub>-PC, Aldrich) were of analytical grade and used as supplied. Sodium dodecylsulphate (SDS, BDH, Special pure), SDS-d25 (Larodan, 98%), sodium chloride (Fluka, *pro analysii*), and deuterium oxide (ICN Biomedicals 99.9%) were used as received. Water was purified in a MilliQ system. Some efforts were spent on selecting the group contributions for the calculation of molecular volumes and scattering length densities. The micelle core is regarded as being composed of fluid hydrocarbons and fluorocarbons, and its volume is calculated by adding contributions from the participating groups as if they were present in pure hydrocarbons and fluorocarbons, neglecting excess volumes in mixtures. From the densities of the normal hydrocarbon (C<sub>6</sub>–C<sub>18</sub>) and fluorocarbon (C<sub>4</sub>–C<sub>10</sub>) liquids at 25 °C as given in Landolt–Börnstein,<sup>32</sup> we calculated the following group contributions:  $V(\text{CH}_2) = 27.1 \text{ \AA}^3$ ,  $V(\text{CH}_3) = 54.4 \text{ \AA}^3$ ,  $V(\text{CF}_2) = 36.6 \text{ \AA}^3$ , and  $V(\text{CF}_3) = 95.1 \text{ \AA}^3$ . The values for the hydrogenous groups are close to those given by Tanford<sup>33</sup> (which were calculated in the same way but without indication of temperature or the source of the data). For the surfactant headgroups and the micelle bound counterions, the relevant volume is that of the water replaced by the group or ion, that is, the partial molar volume. For the pyridinium headgroup, the partial molecular volume of the pyridinium ion in water at infinite dilution was used, given as  $V(\text{Py}^+) = 112 \text{ \AA}^3$ .<sup>34</sup> For the trimethylammonium head group, a volume of  $V(\text{N}(\text{CH}_3)_3^+) = 111 \text{ \AA}^3$  can be deduced from data in the same source.<sup>34</sup> For the sulfate headgroup of SDS, the value of  $\text{HSO}_4^-$  was used,  $V(\text{S}^-) = 62 \text{ \AA}^3$ .<sup>35</sup> The volume of the counterions is again the partial molar volume in water, and assuming  $2/3$  of the counterions to be bound by the micelle, this fraction of the volume is ascribed to bound counterions,  $2/3 V(\text{Cl}^-) = 26 \text{ \AA}^3$  and  $2/3 V(\text{Na}^+) = -7.4 \text{ \AA}^3$ .<sup>35</sup>

The scattering length densities were calculated from atomic scattering lengths and the molecular volumes. The final results were for HFDeP-d5-C  $V_{\text{FS}} = 543.5 \text{ \AA}^3$  and  $\rho_{\text{FS}} = 4.06 \times 10^{10} \text{ cm}^{-2}$ , for C<sub>12</sub>-PC  $V_{\text{HS}} = 490.5 \text{ \AA}^3$  and  $\rho_{\text{HS}} = 0.336 \times 10^{10} \text{ cm}^{-2}$ , and for C<sub>16</sub>-PC  $V_{\text{HS}} = 598.9 \text{ \AA}^3$ ,  $\rho_{\text{HS}} = 0.219 \times 10^{10} \text{ cm}^{-2}$ . For SDS and SDS-d25, the same volume was used,  $V_{\text{S}} = 407 \text{ \AA}^3$ , and the scattering length densities  $\rho_{\text{HS}} = 0.362 \times 10^{10} \text{ cm}^{-2}$  and  $\rho_{\text{DS}} = 6.76 \times 10^{10} \text{ cm}^{-2}$  were used.

**Small Angle Neutron Scattering.** The SANS measurements were performed at the GKSS Research Centre, Geesthacht, Germany.<sup>36</sup> Three different instrumental settings (the sample-to-detector distance was varied from 0.7 to 4.5 m) were used. Experimental data were collected in the interval of the modulus of the scattering vector  $q$  ( $q = (4\pi/\lambda) \sin(\theta/2)$ , where  $\theta$  is the angle between the direct and scattered beam and  $\lambda = 8.2 \text{ \AA}$  is the neutron wavelength) from 0.01 to 0.25  $\text{ \AA}^{-1}$ .

The data were corrected for background scattering, measured for the same salt and H<sub>2</sub>O/D<sub>2</sub>O mixture as used to prepare the surfactant solution, and put on an absolute scale by dividing by the known scattering spectrum of pure H<sub>2</sub>O. The residual incoherent scattering was low, in the order of 0.01  $\text{cm}^{-1}$  or less.

**Data Analysis by Indirect Fourier Transformation.** Data analysis by IFT was performed for  $q > 0.02 \text{ \AA}^{-1}$  where the effects of intermicellar interactions are small.<sup>29</sup> This yields the scattering at zero angle ( $d\Sigma(0)/d\Omega$ ) and the radius of gyration without any presumptions regarding particle shape. The radius of gyration is given by

$$R_g^2 = \frac{\int_0^{D_{\text{max}}} p(r)r^2 dr}{2 \int_0^{D_{\text{max}}} p(r) dr} \quad (6)$$

where  $p(r)$ , the pair distribution function, is approximated by a linear combination of a number of basis functions. The value of  $D_{\text{max}}$ , the limit for the maximum dimension of the particle, was chosen so as to give a stable and smooth solution for the  $p(r)$  function that after Fourier transformation was fitted by a least-squares method to the experimental scattering data. Too much stabilization of the  $p(r)$  solution gives rise to oscillations at high  $q$  values but could not be avoided for the noisy data from measurements close to the match point. The method and program used were those of Glatter<sup>37</sup> as modified by Pedersen,<sup>38</sup> also including correction for instrumental smearing.<sup>39</sup>

## Results

The systems studied were composed as follows:

(1) 20 mM each of C<sub>16</sub>-PC and HFDeP-d5-C in 0.0635 M NaCl, at 25 and 60 °C. Solvent mixtures containing from 0.10 to 1.00 mole fraction D<sub>2</sub>O provided seven contrasts.

(2) 50 mM each of C<sub>12</sub>-PC and HFDeP-d5-C in 0.200 M NaCl at 25 °C. Six solutions with solvent mixtures containing from 0.11 to 1.00 mole fraction D<sub>2</sub>O.

(3) 35 mM each of SDS and SDS-d25 in 0.200 M NaCl at 25 °C. Eight solutions with solvent mixtures containing from 0.10 to 1.00 mole fraction D<sub>2</sub>O.

In system 1, the intermicellar interactions were sufficiently reduced by the addition of 0.063 M salt. In systems 2 and 3, the volume fraction of micellized surfactant was larger, and made the interactions more severe. At 0.100 M NaCl, an interaction peak was still clearly observed in system 2 (weight fraction surfactant 0.043) but was deemed as sufficiently reduced at 0.200 M NaCl. This concentration of salt was used also in system 3.



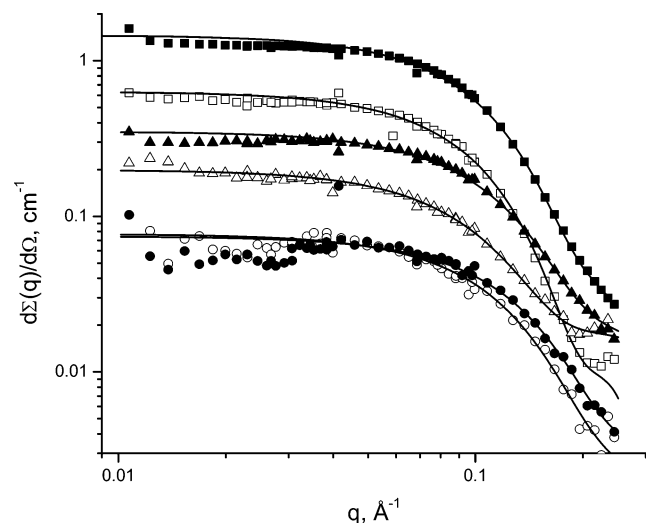


**Figure 1.** SANS data and IFT fits (solid lines) for system 2, 50 mM C<sub>12</sub>PC and 50 mM HFDePC in 0.200 M NaCl. Different contrasts were obtained by variation of D<sub>2</sub>O content in D<sub>2</sub>O/H<sub>2</sub>O: 0.11 (empty squares), 0.3 (empty triangles), 0.4 (empty circles), 0.5 (filled circles), 0.7 (filled triangle), and 1.0 (filled squares).

The concentration of free surfactants in the samples must be estimated. The levels are lower than the free concentration of each surfactant alone, in the presence of the given concentration of counterions, and with repulsive excess interactions larger than the value in an ideal mixture with the other surfactant. The free concentrations of the pure surfactants, as functions of salt and surfactant concentration, can be estimated as discussed recently.<sup>40,41</sup> In system 1, the concentrations should be almost negligible, similar to the values estimated previously for C<sub>16</sub>TAC and HFDePC in 0.100 M NaCl, in the order of 0.1 and 0.2 mM for C<sub>16</sub>TAC and HFDePC, respectively.<sup>12,15</sup> In system 2, the free concentration of HFDePC is negligible. The cmc of C<sub>12</sub>PC in salt free solution is 15 mM. Extrapolating results from Lange<sup>42</sup> according to the methods in ref 40 suggests a value between 2.8 and 1.4 mM in 200 mM NaCl at a surfactant concentration of 100 mM. We have assumed a free concentration of 2 mM in the calculations. For the SDS/SDS-d25 system, the free concentration is less important, since it will be the same for both surfactants, and will only reduce the concentration of surfactant in micelles. From the results in ref 40, the free concentration was chosen as 1 mM for each of the surfactants under the conditions of system 3.

Examples of scattering results (system 2) are shown in Figure 1, together with the resulting IFT fits. The corresponding plots and the  $p(r)$  functions for the other systems are presented as Supporting Information. The values of  $I(0) = d\Sigma(0)/d\Omega$  and the radius of gyration,  $R_g$ , resulting from the IFT analysis are collected in Tables 1–3.

The intensity of scattered neutrons close to the nominal match points is low, and the resulting estimates of  $I(0)$  from the IFT analysis have large error limits. By fitting the results to eq 4, Figure 2, with  $n_m V_m^2$ ,  $\sigma^2$ , and  $\bar{\rho}$  as unknown parameters, reasonable estimates for these parameters were obtained.  $N_{agg}$  was calculated from the first parameter, using the estimated concentration of surfactant in micelles and the surfactant volumes given above. The results are collected in Table 4. Three solvent compositions of system 1 were measured at 60 °C. The results were fitted to eq 4 with  $\bar{\rho}$  fixed at the value obtained from the results at 25 °C.

The first entries in Table 4 are recalculated results from earlier measurements<sup>12</sup> on CTAC and HFDePC, 16.5 mM of each, in

**TABLE 1: Results Obtained from Indirect Fourier Transform Analysis for the System 20 mM C<sub>16</sub>PC and 20 mM HFDePC in 0.0635 M NaCl**

mole fraction D <sub>2</sub> O	$I(0)$ , cm <sup>-1</sup>	$R_g$ , Å	$D_{max}$ , Å	temperature, °C	$\chi^2$ <sup>a</sup>
0.1015	0.317 ± 0.004	19.4 ± 0.2	55	25	1
0.24	0.223 ± 0.004	20.7 ± 0.3	60	25	1
0.374	0.140 ± 0.003	19.6 ± 0.4	60	25	1
0.52	0.170 ± 0.002	17.2 ± 0.2	50	25	2
0.652	0.354 ± 0.004	17.0 ± 0.14	50	25	3
0.80	0.631 ± 0.001	17.4 ± 0.2	50	25	3
1.00	1.290 ± 0.016	17.9 ± 0.14	50	25	4
0.1015	0.190 ± 0.004	17.6 ± 0.3	50	60	1
0.374	0.029 ± 0.002	19.0 ± 0.7	55	60	1
0.652	0.208 ± 0.004	15.0 ± 0.23	50	60	2

<sup>a</sup>  $\chi^2$  for the least-squares fit to the measured data.

**TABLE 2: Results Obtained from Indirect Fourier Transform Analysis for the System 50 mM C<sub>12</sub>PC and 50 mM HFDePC in 0.200 M NaCl at 25 °C**

mole fraction D <sub>2</sub> O	$I(0)$ , cm <sup>-1</sup>	$R_g$ , Å	$D_{max}$ , Å	$\chi^2$ <sup>a</sup>
0.111	0.644 ± 0.008	17.1 ± 0.2	50	3
0.299	0.187 ± 0.003	17.5 ± 0.2	50	3
0.399	0.077 ± 0.003	14.8 ± 0.4	45	1
0.497	0.074 ± 0.002	13.3 ± 0.3	40	1
0.699	0.345 ± 0.005	15.3 ± 0.2	45	3
1.00	1.48 ± 0.02	16.7 ± 0.2	50	4

<sup>a</sup>  $\chi^2$  for the least-squares fit to the measured data.

**TABLE 3: Results Obtained from Indirect Fourier Transform Analysis for the System 35 mM SDS and 35 mM SDS-d25 in 0.200 M NaCl at 25 °C**

mole fraction D <sub>2</sub> O	$I(0)$ , cm <sup>-1</sup>	$R_g$ , Å	$D_{max}$ , Å	$\chi^2$ <sup>a</sup>
0.100	0.57 ± 0.01	16.7 ± 0.2	45	3
0.200	0.353 ± 0.006	17.1 ± 0.02	50	3
0.300	0.197 ± 0.003	17.3 ± 0.2	50	2
0.500	0.0144 ± 0.009	17.3 ± 0.3	45	1
0.640	0.0137 ± 0.0010	12 ± 1	35	1
0.780	0.1104 ± 0.0019	15.3 ± 0.2	45	2
0.900	0.280 ± 0.005	16.1 ± 0.02	45	3
1.00	0.516 ± 0.007	16.4 ± 0.1	45	4

<sup>a</sup>  $\chi^2$  for the least-squares fit to the measured data.

100 mM NaCl. We have used new values for the molar volumes of the surfactants, as estimated above, and also used a different parametrization in the fitting to eq 4. The results for the systems with pyridinium and trimethylammonium headgroups are fairly similar. The composition distribution at 25 °C seems to be broader in C<sub>16</sub>PC/HFDePC, but the change in  $\sigma$  by a factor of almost 2 with a change in temperature from 25 to 60 °C is very large, and signals some caution. We return to this question below. The reduction of the width from system 1 with C<sub>16</sub>PC to system 2 with C<sub>12</sub>PC is according to the expectation: a reduction of the length of hydrocarbon (or the fluorocarbon) chains reduces the interaction energy. In the ideal mixture of system 3, the width is even further reduced.

With respect to the aggregation numbers, a direct comparison with literature values can only be made in the case of SDS in system 3. The aggregation numbers appear rather low. Earlier studies by SANS<sup>25</sup> and other methods<sup>41</sup> suggest a value close to 100 under conditions as in system 3. In all systems, the results suggest roughly globular micelles, and we expect as observed larger aggregation numbers with the long chain C<sub>16</sub> surfactants than with the C<sub>12</sub> surfactant. A close look at the scattering curves in Figure 1 and for system 1 in Supporting Information Figure 1S (or Figure 6) gives some indication of a change of size with the contrast. In both cases, the curves from contrast where the hydrogenous component contributes little to the scattering seem to suggest larger micelles than the corresponding curves from

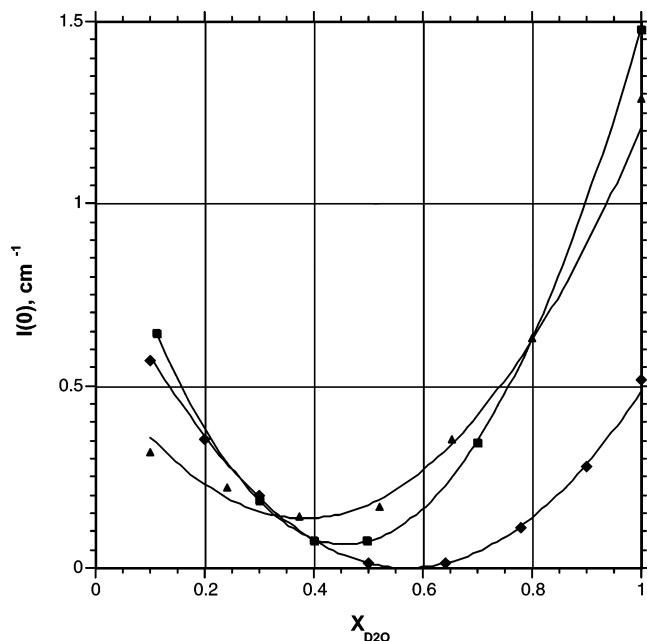


**Figure 2.** Parabolas, according to eq 4, fitted to the  $I(0)$  results for systems 1–3. The nominal match point increases and the intensity at the match point decreases from  $C_{16}$ PC/HFDePC (triangles), over  $C_{12}$ PC/HFDePC (squares), to SDS/SDS-d25 (diamonds).

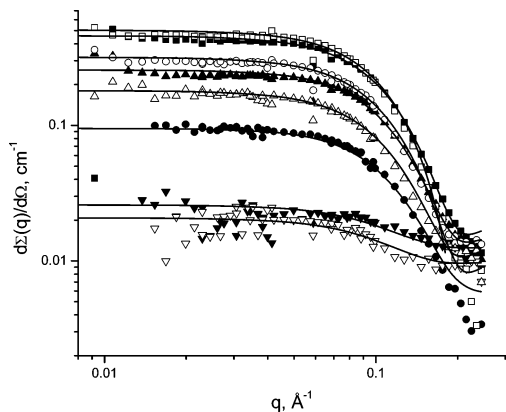


**Figure 3.** SANS data and fits to a one-shell model of oblate ellipsoids of rotation with effective hard-sphere interactions and a Gaussian composition distribution (solid lines) for mixture of SDS (35 mM) and SDS-d25 (35 mM) in 0.2 M NaCl at different contrasts.  $x_{D_2O} = 1$  (filled squares), 0.9 (filled triangles up), 0.78 (filled circles), 0.64 (filled triangles down), 0.50 (open triangles down), 0.30 (open triangles up), 0.20 (open circles), and 0.10 (open squares).

the contrast that matches the fluorinated surfactant. We will return to these points in the direct modeling section.

### Modeling of Scattering Data

The IFT analysis together with theoretical considerations (see the Discussion section) gives us guidance for direct modeling

**TABLE 4: Micelle Aggregation Number, Width of Composition Distribution, and  $x_{\min}$ , Mole Fraction of  $D_2O$  in the Solvent Giving the Lowest Intensity of Neutron Scattering, for the Systems Studied, Using  $I(0)$  Obtained from IFT (Compare to Table 5)**

system	$N_{\text{agg}}$	$\sigma$	$x_{\min}$	$(x_{\min})_{\text{calcd}}$
$C_{16}$ TAC/HFDePC <sup>a</sup> (25 °C)	$83.5 \pm 0.8$	$0.31 \pm 0.003$	$0.35 \pm 0.002$	0.34
$C_{16}$ TAC/HFDePC <sup>a</sup> (60 °C)	$61 \pm 1.5$	$0.19 \pm 0.01$		0.34
1, $C_{16}$ PC/HFDePC (25 °C)	$79 \pm 0.6$	$0.37 \pm 0.003$	$0.38 \pm 0.01$	0.375
1, $C_{16}$ PC/HFDePC (60 °C)	$71 \pm 1.2$	$0.19 \pm 0.01$		0.375
2, $C_{12}$ PC/HFDePC (25 °C)	$63.5 \pm 0.6$	$0.22 \pm 0.003$	$0.46 \pm 0.001$	0.42
3, SDS/SDS-d25 (25 °C)	$79 \pm 0.7$	$0.006 \pm 0.030$	$0.57 \pm 0.001$	0.59

<sup>a</sup> Results from ref 12, recalculated.

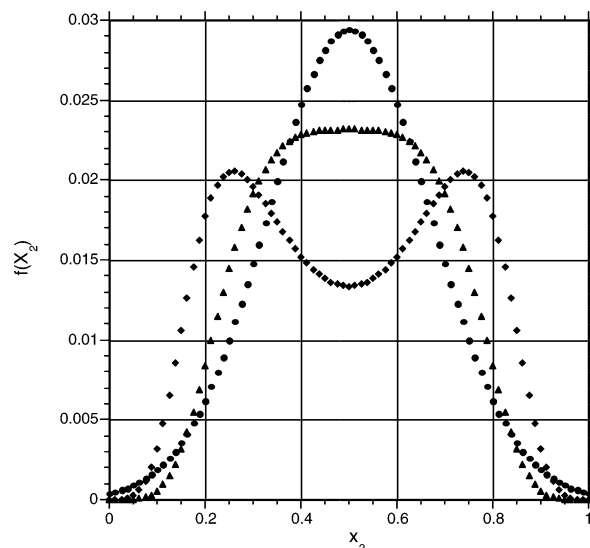


**Figure 4.** Micelle composition distributions for models of system 2,  $C_{12}$ PC/HFDePC. A Gaussian distribution with  $\sigma = 0.17$ , as obtained in the fitting (filled circles) compared to a distribution according to the regular solution lattice (RSL) model, as discussed below, calculated for an aggregation number of 80 and the same  $\sigma$  value (filled triangles). The bimodal distribution (filled diamonds) is calculated according to the RSL model with  $N_{\text{agg}} = 80$  and  $\sigma = 0.22$ , as obtained in the IFT fitting. This distribution was prescribed in the RSL fitting to the data for system 2.

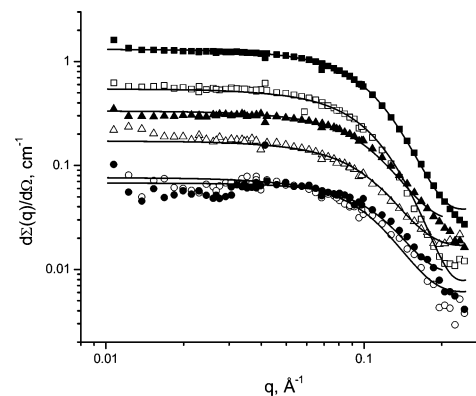


**Figure 5.** SANS data and model fits (prolate ellipsoids, RSL composition distribution, solid lines) for system 2, 50 mM  $C_{12}$ PC and 50 mM HFDePC in 0.200 M NaCl. Different contrasts were obtained by variation of  $D_2O$  content in  $D_2O/H_2O$ : 0.11 (empty squares), 0.3 (empty triangles), 0.4 (empty circles), 0.5 (filled circles), 0.7 (filled triangles), and 1.0 (filled squares).

of the scattering curves measured at different contrasts. The simplest situation is the case of h-SDS and d-SDS where mixed micelles with a narrow composition distribution are expected. Bergström and Pedersen<sup>25</sup> have performed comprehensive SANS studies of SDS at several concentrations and with added salt. They found that at concentrations of salt and surfactant as

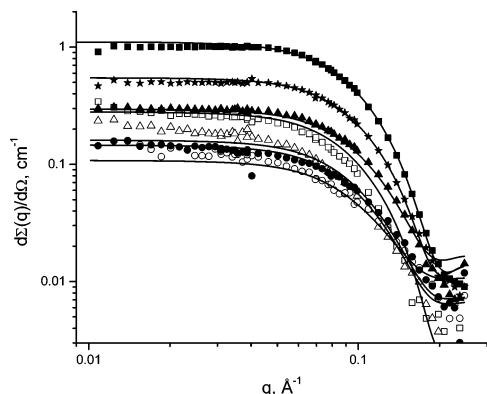


**Figure 6.** SANS data and model fit (ellipsoid of revolution with RSL composition distribution) for system 1, C<sub>16</sub>PC/HFDePC in 0.063 M NaCl at different contrasts.  $x_{D_2O} = 1$  (filled squares), 0.8 (stars), 0.65 (filled triangles), 0.52 (filled circles), 0.374 (open circles), 0.24 (open triangles), 0.10 (open squares).

in the present study the micelles could be modeled as uniform ellipsoids of revolution, without separate head group shells. We applied this model with an effective excluded volume interaction, within the decoupling approximation.<sup>24</sup> The scattering intensities are written as

$$\frac{d\Sigma}{d\Omega}(q) = n_m V_m^2 [\langle F(r, q)^2 \rangle_o \int (\rho - \rho_s)^2 f(\rho) d\rho + \langle \langle F(r, q) \rangle_o \int (\rho - \rho_s) f(\rho) d\rho \rangle_o^2 (S(q) - 1)] + B_{inc} \quad (7)$$

where  $F(r, q)$  is the form factor of the micelles and  $\langle \dots \rangle_o$  denotes the orientation average. The expression for the orientation averaged form factor is found in the literature.<sup>25,43</sup>  $S(q)$  is the structure factor which reflects interactions among the micelles, and  $B_{inc}$  is the residual incoherent scattering. The composition distribution of the micelles gives a scattering length density distribution,  $f(\rho)$ . The integration is performed over all of the scattering length densities in the full composition range, from pure surfactant 1 to pure surfactant 2. For mixed micelles of d-SDS and h-SDS, a Gaussian composition distribution was chosen. The dispersion around the average value of  $\rho$  was fitted to match the experimental data.

For  $S(q)$ , we used an effective hard-sphere expression as calculated with the Percus–Yevick approximation for the closure relation.<sup>43,44</sup>

$$S(q) = \frac{1}{1 + 24\eta_{HS}G(qR_{HS})/qR_{HS}} \quad (8)$$

where  $\eta_{HS}$  is the hard-sphere volume fraction and  $R_{HS}$  is the effective hard-sphere radius. The detailed expression of the function  $G(qR_{HS})$  can be found in the literature.<sup>43</sup>  $R_{HS}$  is allowed to take on a value larger than  $R_{eq}$ , the radius of a sphere with the same volume as the micelle. The residual electrostatic

interactions that are not completely screened by the addition of salt and the increased range of the hard-sphere interactions due to the departure from spherical shape are intended to be accounted for by this scaling  $R_{HS}$  and  $\eta_{HS}$ .

All together, five parameters were used to describe simultaneously eight scattering curves plus eight residual incoherent scatterings,  $B_{inc}$ , one for each curve. The model can satisfactorily describe the data (Figure 3, Table 5). The value of  $\chi^2$  does not alone measure the goodness of fit; it can only be used to compare the fit of different models. Using a monodisperse core–shell sphere as a model, with only the core having a composition-dependent scattering length density, the fit was almost as good— $\chi^2 = 6$  as compared to 5.5—but the shell thickness was poorly defined, and the scattering length density of the shell was assigned a value close to the scattering length density at the match point, or in other words, a value close to the average scattering length density of the core.

The modeled scattering curves shown in Figure 3 seem to agree better with the experimental results than the corresponding curves from the IFT analysis (Supporting Information Figure 3S), and the calculated aggregation number of 94 is in better accord with the expectations. The width of the Gaussian composition distribution is too small (as also the value obtained from the analysis using eq 4) and cannot be reconciled with the expectation of a binominal distribution.

Application of the model with spherical core–shell micelles and a composition distribution of Gaussian type to the scattering data of the system C<sub>12</sub>PC/HFDePC gave again unrealistic values of the parameters. A model of monodisperse spheres with a Gaussian composition distribution was also tested, with results as shown in Table 5 for comparison with the fitting to the regular solution lattice (RSL) model. The width of the Gaussian distribution is obtained as 0.17. This Gaussian distribution is so broad that it is somewhat truncated on the composition scale from 0 to 1; see Figure 4 where it is compared to a RSL model of the same width.

We have also fitted the data from system 2 to a model with prolate micelles (semi-axis  $R$ ,  $R$ ,  $\gamma R$  having a prescribed composition distribution, a RSL distribution with  $\sigma = 0.22$  (shown in Figure 4) as obtained from the IFT analysis using eq 4. The integral quality of fit was better than in the previous model. The aggregation number was obtained as  $86 \pm 3$ .

Mixtures of C<sub>16</sub>PC/HFDePC were fitted by a model with ellipsoids of revolution having a composition distribution from RSL, calculated for  $\sigma = 0.37$  and  $N_{agg} = 100$  (represented in Figure 7 below; the fact that the aggregation number calculated from the parameters at best fit is somewhat lower does not markedly affect the composition distribution). The integral quality of fit is slightly better ( $\chi^2 = 5$ ), and the aggregation number obtained as  $88 \pm 3$ .

The experimental data and the fitted models with prolate micelles and RSL composition distributions are shown in Figures 5 and 6, for systems 2 and 1, respectively. In both cases,

**TABLE 5: Values of the Parameters  $\gamma$ ,  $R_t$ ,  $\sigma$ ,  $R_{HS}/R_{eq}$ , and  $B_{inc}$ , Obtained from Direct Simultaneous Fit to Contrast Variation SANS Data of Mixtures, Together with  $\chi^2$  for the Fit, and  $N_{agg}$  Calculated from Micelle and Surfactant Volumes**

	3, SDS/SDS-d25 Gaussian, oblate	2, C <sub>12</sub> PC/HFDePC, Gaussian, sphere	2, C <sub>12</sub> PC/HFDePC, RSL, $\sigma = 0.22$ , $N_{agg} = 80$	1, C <sub>16</sub> PC/HFDePC, RSL, $\sigma = 0.37$ , $N_{agg} = 100$
$\gamma$	$0.73 \pm 0.1$		$1.7 \pm 0.1$	$1.5 \pm 0.1$
$R_t$ , Å	$23.2 \pm 0.5$	$21.7 \pm 0.3$	$18.1 \pm 0.5$	$20.0 \pm 0.5$
$\sigma$	$0.006 \pm 0.003$	0.17		
$R_{HS}/R_{eq}$	$1.4 \pm 0.1$	$1.6 \pm 0.1$	$1.7 \pm 0.2$	$1.8 \pm 0.2$
$B_{inc}$ , cm <sup>-1</sup>	0.005–0.014	0.005–0.02	0.005–0.015	0.005–0.01
$\chi^2$	5.5	9	6	5
$N_{agg}$	$94 \pm 4$	$83 \pm 4$	$86 \pm 3$	$88 \pm 3$

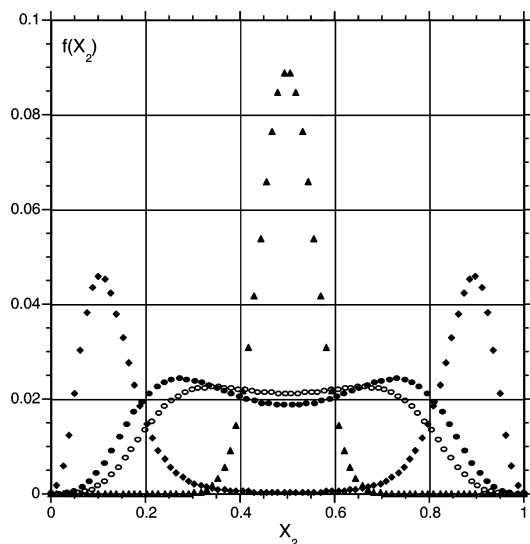


**Figure 7.** Micelle composition distributions for regular solution models. The models were chosen so as to correspond to the systems in Table 4. System 1, at 25 °C,  $N_{\text{agg}} = 79$ ,  $\alpha = 2.65$ ,  $\sigma = 0.373$  (filled diamonds); system 2, 25 °C,  $N_{\text{agg}} = 63$ ,  $\alpha = 2.12$ ,  $\sigma = 0.219$  (filled circles); system 1, 60 °C,  $N_{\text{agg}} = 71$ ,  $\alpha = 2.04$ ,  $\sigma = 0.194$  (open circles); ideally mixed system,  $N_{\text{agg}} = 79$ ,  $\alpha = 0.00$ ,  $\sigma = 0.0563$  (filled triangles).

the models fit the data somewhat better than in the corresponding IFT analysis, see Supporting Information Figure 1S and Figure 1, respectively, as can be expected when micellar interactions are taken into account. There seem to be some systematic deviations that might indicate a composition-dependent size variation. To check this point, we have separately fitted the data for the contrasts closest to those of the pure fluorinated and hydrogenous surfactants with the model of ellipsoid of revolution. In  $C_{16}\text{PC}/\text{HFDePC}$ , the results for the sample with  $x_{\text{D}_2\text{O}} = 0.65$  indicate a prolate ellipsoid of revolution with semi-axis 20, 20, 28 Å and with  $x_{\text{D}_2\text{O}} = 0.10$ , where the fluorinated surfactant dominates, the objects are more elongated, 20, 20, 40 Å. In the mixture of  $C_{12}\text{PC}/\text{HFDePC}$ , the result at  $x_{\text{D}_2\text{O}} = 0.70$  was 18, 18, 25 Å as compared to 18, 18, 34 Å at  $x_{\text{D}_2\text{O}} = 0.11$ . This indicates a considerable change of size with composition. The aggregation numbers change by a factor of about 1.6 in system 1 and 1.4 in system 2.

The main conclusion from the direct modeling is that we are able to fit the experimental data with a composition distribution suggested from IFT analysis and the regular solution lattice model.

## Discussion

Deviations between the solvent compositions at the calculated nominal match points and at the smallest scattered intensity will be considered first. Micelle composition distributions will then be discussed, in particular what distributions are expected within the regular solution model for micelles of constant size and how the width,  $\sigma$ , of the distribution varies with the interaction parameter.

In order to understand the consequences of a situation where the micelle aggregation number varies with the composition, we have considered a model system with only two micelle types, aggregation numbers  $N_1$  and  $N_2$ , respectively, with different compositions, instead of a broad composition distribution. (A more general treatment is given in the work of Avdeev.<sup>30</sup>) Assuming symmetry around a mean composition of 0.5, the compositions of the two types of micelles are fixed by the value

of  $\sigma$ . Ignoring intermicellar interactions, the scattering intensity should be given by

$$\frac{d\Sigma}{d\Omega}(0) = n_1 V_1^2 (\rho_1 - \rho_s)^2 + n_2 V_2^2 (\rho_2 - \rho_s)^2 \quad (9)$$

where subscripts 1 and 2 refer to the two types of micelles and  $\rho_s$  is the scattering length density of the solvent. The minimum of the scattered intensity is obtained at a scattering length density of the solvent mixture determined by

$$\rho_{s,\text{min}} = \frac{n_1 V_1^2 \rho_1 + n_2 V_2^2 \rho_2}{n_1 V_1^2 + n_2 V_2^2} \quad (10)$$

The volume of a micelle depends on the aggregation number, composition, and surfactant volumes. The number of micelles is related to the aggregation numbers. For symmetrical demixing of a 50:50 mixture, we find  $n_1 N_1 = n_2 N_2$  (it follows that  $n_1 V_1 = n_2 V_2$  if the surfactant volumes are equal; in our systems, they differ by less than 10% for the pure surfactants). The scattering length densities of the micelles are calculated from the composition and the volumes and scattering length densities of the surfactants.

Using constants as for system 2 and assuming that the aggregation number of the fluorocarbon rich micelles was twice as large as that of the hydrocarbon rich micelles, we find that the minimum should occur at about 10% larger scattering length density than at the nominal match point. The deviation between observed and calculated match points was in this range for system 2. In system 1, however, where the large  $\sigma$  value implies a larger difference between the scattering length densities of the micelles, a similar size difference would give a much larger deviation. The fact that no such difference is observed between the scattering length density at the nominal match point and at the minimum in the  $I(0)$  curve indicates that the change of size with composition is smaller than what the direct modeling seems to imply.

Note that we do not suggest that in system 2 a demixing into just two types of micelles has occurred. As will be made clear below, the main conclusion is that this system is best represented by a broad distribution of compositions, which may be slightly bimodal. The added conclusion from the considerations of the deviation between the calculated and observed match points, from the direct modeling, and from the change of the pair distance distributions with the contrast, is that there might be a size variation coupled to the composition variation within this broad distribution. A reason for why such a composition-dependent difference in the micelle sizes would be found in this system could be that micelles of pure  $C_{12}\text{PC}$  remain globular even at high ionic strength, whereas micelles of HFDePC (and to a lesser degree micelles of  $C_{16}\text{PC}$  in system 1) have a tendency to grow into large, even rod shaped, micelles at high salt concentration. A problem, however, is that the aggregation numbers of the  $C_{12}\text{PC}$  rich micelles would be somewhat small—about 65 from the direct modeling—which is smaller than would be expected even for pure  $C_{12}\text{PC}$  micelles at this salt concentration.

Let us now consider the implications for the micelle composition distributions of the determined values of the width of the distribution. Equation 22 in ref 6 allows the calculation of micelle size distributions in a two-dimensional lattice model consistent with the regular solution results, assuming equal size of the lattice cells (i.e., equal size of the surfactants; in systems



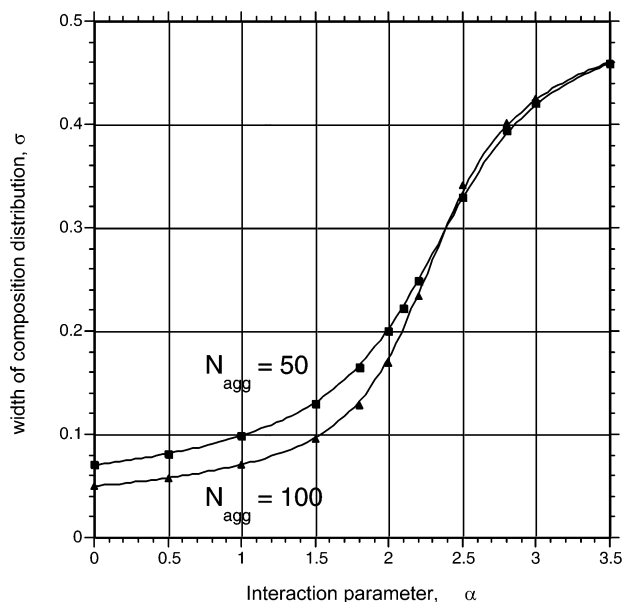


**Figure 8.** Standard deviation calculated from the composition distributions for the regular solution model mixed micelles with aggregation numbers of 50 and 100. The solid lines are guides to the eye.

1 and 2, the two surfactants differ by about 10% in volume) and equal size of the micelles.

Figure 7 shows the fraction of micelles,  $f(x_2)$ , with a fraction,  $x_2$ , of surfactants of type 2 for micelles with aggregation numbers and values of the regular solution interaction parameter chosen to represent systems 1–3. The interaction parameter varies from the ideal case to a positive value of  $\alpha = 2.65$ . Note that the distribution for  $\alpha = 2.04$  shows a distinct minimum at  $x_2 = 0.5$ ; a shallow minimum is also found for  $\alpha = 2.00$ , because of the finite size of the micelles; the critical value of  $\alpha = 2$  applies to an infinite lattice.<sup>6</sup>

The standard deviation,  $\sigma$ , of the composition distributions varies with the interaction parameter,  $\alpha$ , in a way that depends on the aggregation number. In Figure 8, calculated  $\sigma$  values for  $N_{\text{agg}} = 50$  and 100 are shown. The aggregation number has the largest influence on the standard deviation at interaction parameters smaller than 2; at large values of the interaction parameter,  $\sigma$  approaches the maximum value of 0.5 for totally demixed micelles, independent of the aggregation number. Note also that  $\sigma$  increases slowly with the interaction parameter for  $\alpha < 1.5$  and much more rapidly in the range  $2 < \alpha < 3$ . The change becomes very slow at zero and negative values of the interaction parameter (not shown).

From the relationship described in Figure 8 and the results collected in Table 4, we conclude that the composition distributions for systems  $C_{16}\text{TAC}/\text{HFDePC}$  and  $C_{16}\text{PC}/\text{HFDePC}$  at 25 °C are clearly bimodal but still with appreciable concentrations of fully mixed micelles. At 60 °C, the  $\sigma$  values are the same for both systems and correspond to broad distributions that at most are slightly bimodal. The interaction parameters, as obtained from Figure 8, are 2.4 and 2.62, respectively, for the two systems at 25 °C, and the ratio of the interaction parameters at the two temperatures are 1.17 and 1.28, respectively, for  $C_{16}\text{TAC}/\text{HFDePC}$  and  $C_{16}\text{PC}/\text{HFDePC}$ , substantially larger than the ratio, 1.12, of the absolute temperatures. We have to consider now if the relatively large difference in interaction parameters between the two systems at the lower temperature really is correct and if the change from the pyridinium headgroup to the trimethylammonium headgroup, with the same charge and similar volume, really would give such a strong change of the

interactions. Strong evidence against such a proposition is given by the facts that the interactions are similar at the higher temperature and that the change of the interaction parameter in the  $C_{16}\text{PC}$  system is much larger than what could be explained by the temperature change alone (i.e., the interaction free energy,  $w$ , and/or the number,  $z$ , of nearest neighbors in the lattice must also change). It seems likely, therefore, that the estimates of the  $\sigma$  values are more uncertain than what the error limits indicate, possibly as a result from uncertainties in the  $I(0)$  values due to remaining intermicellar interactions.

For the ideally mixed system, SDS/SDS-d25, the width is much smaller than what zero interaction energy would suggest. We have no good explanation for this inconsistency.

Let us now consider to what extent the composition distributions discussed above can be looked upon as representative for the real systems. The easy answer is that the real systems probably have quite different distributions. The lattice models are oversimplified, not only with respect to the assumed constant volumes of the cells but also regarding the interactions between the surfactants. The conformations of the surfactants, their orientations, and varying separation distances lead to complicated interactions that cannot be captured by a single nearest neighbor interaction parameter. Real systems will not normally show the symmetry expressed by the simple lattice theories.

Still, the regular solution theory has been found useful to characterize nonideal mixed systems, with respect to the change of the cmc for surfactant mixtures, and the possibility of phase separation (or a demixing in the micellar case). In a similar way, lacking detailed information, it may be of some value to look upon the micelle composition distributions calculated within the regular solution framework as giving a rough picture of the distributions in the systems under study. There are, however, some specific aspects of the regular solution variant of the lattice models that require further consideration.

The regular solution model is a mean field theory: it is assumed that the surfactants are randomly distributed over the lattice, independent of the interactions between them. This is of course not a good approximation for strong interactions that lead to phase separation, or to clustering of the surfactants in domains, as have been suggested to occur in some micellar systems.<sup>16,17</sup> From exact lattice calculations (available for 50:50 mixtures of a square lattice)<sup>7,46</sup> it is known that the critical value of the interaction parameter,  $\alpha \equiv zw/kT$ , depends on the lattice type and is equal to 3.53 for  $z = 4$  (a square lattice) which is appreciably larger than the critical value of 2 from the regular solution model. Furthermore, from numerical solutions for finite lattices, such as micelles, it is also known that the critical value decreases strongly with decreasing lattice size.<sup>6</sup> Also, the composition distributions are strongly affected, in particular around the critical point. At similar distances from the critical point, however, the composition distributions from the mean field approximation and an exact (numerical) lattice calculation are more similar, although still different. The mean field theory gives narrower distributions in the vicinity of the critical point.<sup>6</sup>

The fact that the value of the critical interaction parameter in the regular solution model is lower than the exact value could be a problem. In the experimental practice, however, the value of  $\alpha$  is determined from the activity coefficients, as obtained for instance from the variation of the free surfactant concentrations with the average micelle composition. In the regular solution model,  $\alpha$  is thus obtained from eq 2. In more refined theories, the activity factors have a much more complicated dependence on  $z$  and  $w$ . Thus, some of the effects of the

nonrandomness of the surfactant distributions on the lattice are accounted for in the value of  $\alpha$  obtained when the regular solution model is applied. The excess energy,  $w$ , would then be temperature dependent, and direct determinations of  $w$ , for example, from calorimetric measurements, would give results inconsistent with the results from cmc determinations.<sup>46,47</sup> We propose that the value of  $\sigma$  for the composition distribution, via the regular solution results in Figure 8, gives a value of the interaction parameter that is in better accord with the value from cmc determinations, and gives a reasonable idea about the composition distribution from Figure 7. Note, however, that the relationship between the composition distribution and the deviation of the free surfactant concentrations from that of ideal mixing, can only be expected to be valid for short range interactions; the electrostatic interactions in solutions of charged surfactants at low ionic strength can be expected to have a much stronger effect on the free surfactant concentrations than on the distribution of the surfactants among the micelles.<sup>11</sup>

## Conclusions

We have determined the width,  $\sigma$ , of micelle composition distributions in systems composed of micelles formed by two surfactants, from SANS contrast variation measurements. We obtain reasonable results, indicating broad distributions in systems composed of long chain hydrocarbon-fluorocarbon surfactants, somewhat less broad at higher temperature or with a shorter hydrocarbon chain, and a very narrow distribution for an ideally mixed system. The measurements allow the estimation of only a single parameter related to the composition distribution. By invoking the regular solution model, this parameter,  $\sigma$ , can be related to the interaction parameter,  $\alpha$ , of the regular solution model, and to distinct micelle composition distributions. Some direct modeling performed with a composition distribution imposed, including effects of micellar interactions, and allowing for prolate or oblate micelles shapes, can mimic the experimental results. Modeling of individual scattering curves for selected contrasts gave indications on a change of size with composition.

**Acknowledgment.** The project was supported by the Swedish Research Council (VR) and by the Carl Trygger Foundation and by the European Commission under the 6th Framework Programme through the Key Action: Strengthening the European Research Area, Research Infrastructures. Contract no: RII3-CT-2003-505925.

**Supporting Information Available:** Figures showing neutron scattering data and pair distance distribution functions,  $p(r)$ . This material is available free of charge via the Internet at <http://pubs.acs.org>.

## References and Notes

- Holland, P. M. In *Mixed Surfactant Systems*; Holland, P. M., Rubingh, D. N., Eds.; ACS Symposium Series 501; American Chemical Society: Washington, DC, 1992; pp 31–44.
- Jönsson, B.; Lindman, B.; Holmberg, K.; Kronberg, B. *Surfactant and Polymers in Aqueous Solution*; Wiley: Chichester, England, 1998; Chapter 5.
- Nishikido, N. In *Mixed Surfactant Systems*; Ogino, K., Abe, M., Eds.; Surfactant Science Series, Vol. 46; Marcel Dekker: New York, 1993; p 23.
- Graciaa, A. P.; Lachaise, J.; Schechter, R. S. In *Mixed Surfactant Systems*; Ogino, K., Abe, M., Eds.; Surfactant Science Series, Vol. 46; Marcel Dekker: New York, 1993; p 63.
- Motomura, K.; Aranato, M. In *Mixed Surfactant Systems*; Ogino, K., Abe, M., Eds.; Surfactant Science Series, Vol. 46; Marcel Dekker: New York, 1993; p 99.
- Barzykin, A. V.; Almgren, M. *Langmuir* **1996**, *12*, 4672.
- Hill, T. L. *An introduction to statistical thermodynamics*; Addison Wesley: Reading, PA, 1960.
- Clint, J. H. *J. Chem. Soc., Faraday Trans. 1* **1975**, *71*, 1327.
- Lange, H. *Kolloid Z.* **1953**, *13*, 96. Shinoda, K. *J. Phys. Chem.* **1954**, *58*, 541.
- Almgren, M.; Hansson, P.; Wang, K. *Langmuir* **1996**, *12*, 4672.
- Almgren, M.; Wang, K.; Asakawa, T. *Langmuir* **1997**, *13*, 4535.
- Almgren, M.; Garamus, V. M. *J. Phys. Chem. B* **2005**, *109*, 11348.
- Murkerjee, P.; Mysels, K. J. In *Colloidal Dispersions and Micellar Behavior*; Mittal, K. L., Ed.; American Chemical Society: Washington, DC, 1975; p 239.
- Funasaki, N. In *Mixed Surfactant Systems*; Ogino, K.; Abe, M., Eds.; Surfactant Science Series, Vol. 46; Marcel Dekker: New York, 1993; p 145.
- Kadi, M.; Hansson, P.; Almgren, M.; Bergström, M.; Garamus, V. M. *Langmuir* **2004**, *20*, 3933.
- Kadi, M.; Hansson, P.; Almgren, M.; Furó, I. *Langmuir* **2002**, *18*, 9243.
- Nordstierna, L.; Furo, I.; Stilbs, P. *J. Am. Chem. Soc.* **2006**, *128*, 6704.
- Burkitt, S. J.; Ottewill, R. H.; Hayter, J. B.; Ingram, B. T. *Colloid Polym. Sci.* **1987**, *265*, 628.
- Caponetti, E.; Chilura, Martino, D.; Floriano, M. A.; Triolo, R. *Langmuir* **1993**, *9*, 1193.
- Pedone, L.; Chilura Martino, D.; Caponetti, E.; Floriano, M. A.; Triolo, R. *J. Phys. Chem. B* **1997**, *101*, 9525.
- Ravey, J. C.; Gherbi, A.; Stébé, M. *J. Prog. Colloid Polym. Sci.* **1989**, *79*, 272.
- Hayter, J. B.; Penfold, J. *Colloid Polym. Sci.* **1983**, *261*, 1022.
- Hayter, J. B. In *Physics of Amphiphiles, Micelles, Vesicles and Microemulsions*; Degiorgio, V., Corti, M., Eds.; North-Holland: Amsterdam, The Netherlands, 1992.
- Koltarchyk, M.; Chen, S. H. *J. Chem. Phys.* **1983**, *79*, 2461.
- Bergström, M.; Pedersen, J. S. *J. Phys. Chem. Chem. Phys.* **1999**, *1*, 4437.
- Bergström, M.; Pedersen, J. S. *J. Phys. Chem. B* **1999**, *103*, 8502.
- Penfold, J.; Staples, E.; Thompson, L.; Tucker, I.; Hines, J.; Thomas, R. K.; Lu, J. R. *Langmuir* **1995**, *11*, 2496.
- Penfold, J.; Staples, E.; Thompson, L.; Tucker, I.; Hines, J.; Thomas, R. K.; Lu, J. R.; Warren, N. *J. Phys. Chem. B* **1999**, *103*, 5204.
- Glatter, O. In *Small Angle X-ray Scattering*; Glatter, O., Kratky, O., Eds.; Academic Press: London, 1982.
- Avdeev, M. V. *J. Appl. Crystallogr.* **2007**, *40*, 56.
- Asakawa, T.; Hisamatsu, H.; Miyagishi, S. *Langmuir* **1995**, *11*, 478.
- Thermodynamic Properties of Organic Compounds and Mixtures*; Landolt-Börnstein Online; Springer-Verlag: Berlin, 2006; Vol. 8B.
- Tanford, C. *The Hydrophobic Effect*; Wiley: New York, 1980.
- Laliberté, L. H.; Conway, B. E. *J. Phys. Chem.* **1970**, *74*, 4116.
- Marcus, Y. *J. Chem. Soc., Faraday Trans.* **1993**, *89*, 713.
- Stuhrmann, H. B.; Burkhard, N.; Dietrich, G.; Junemann, R.; Meerwin, W.; Shmitt, M.; Wadzack, J.; Willumeit, R.; Zhao, J.; Nierhaus, K. H. *Nucl. Instrum. Methods Phys. Res., Sect. A* **1995**, *356*, 124.
- Glatter, O. *J. Appl. Crystallogr.* **1977**, *10*, 415.
- Hansen, S.; Pedersen, J. S. *J. Appl. Crystallogr.* **1991**, *24*, 541.
- Pedersen, J. S.; Posselt, D.; Mortensen, K. *J. Appl. Crystallogr.* **1990**, *23*, 321.
- Bales, B. L.; Messina, L.; Vidal, A.; Peric, M.; Nascimento, O. R. *J. Phys. Chem. B* **1998**, *102*, 10347.
- Quina, F. H.; Nassar, P. M.; Bonilha, J. B. S.; Bales, B. L. *J. Phys. Chem. B* **1995**, *99*, 17028.
- Lange, H. *Kolloid Z.* **1951**, *121*, 66.
- Pedersen, J. S. *Adv. Colloid Interface Sci.* **1997**, *70*, 171.
- Kinning, D. J.; Thomas, E. L. *Macromolecules* **1984**, *17*, 1712.
- Percus, J. K.; Yevick, G. *J. Phys. Rev.* **1958**, *110*, 1.
- Guggenheim, E. A. *Mixtures*; Oxford University Press: Oxford, U.K., 1952.
- Hoffmann, H.; Pössnecker, G. *Langmuir* **1994**, *10*, 381.